Supporting Information

Doping and Interface Engineering in Sandwich $Ti_3C_2T_X/MoS_{2-x}P_x$ Heterostructure for Efficient Hydrogen Evolution

Xiaojun Zeng,[a,*,1] Derong Duan,[a,1] Xiaofeng Zhang,[b,*] Xiaohong Li,[a] Kai Li,[a] Ronghai Yu,[c] Martin Moskovits[d]

[a] School of Materials Science and Engineering, Jingdezhen Ceramic University, Jingdezhen 333403, China

[b] Guangdong Academy of Science, Guangdong Institute of New Materials, National Engineering Laboratory for Modern Materials Surface Engineering Technology, The Key Lab of Guangdong for Modern Surface Engineering Technology, Guangzhou, 510650, China

[c] School of Materials Science and Engineering, Beihang University, Beijing, 100191, China

[d] Department of Chemistry and Biochemistry, University of California Santa Barbara, Santa Barbara, CA, 93106, United States

* Corresponding author, E-mail: zengxiaojun@jci.edu.cn (X.J. Zeng), zxf200808@126.com (X.F. Zhang)

[1] These authors contributed equally to this work.

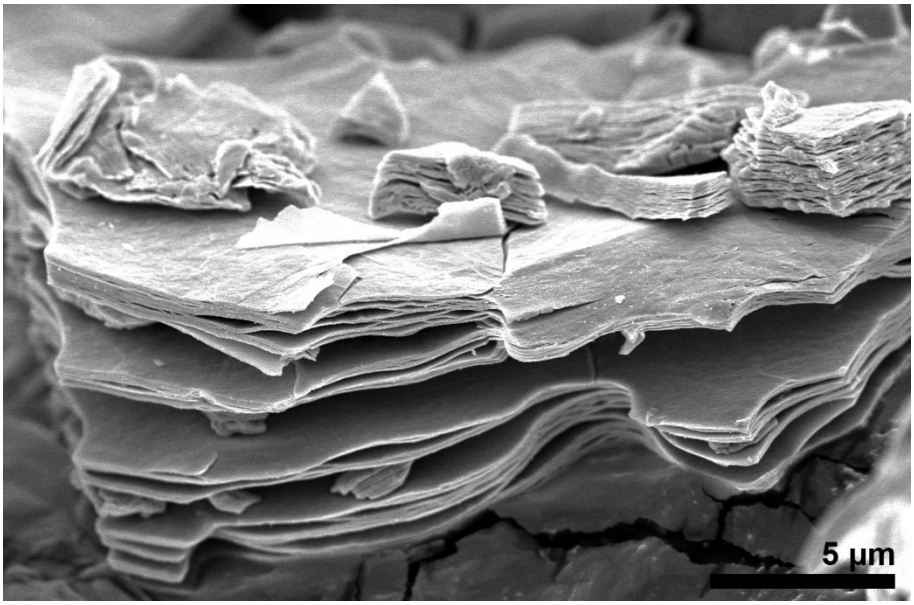

Figure S1. SEM images of 2D layered $Ti_3C_2T_x$ MXene.

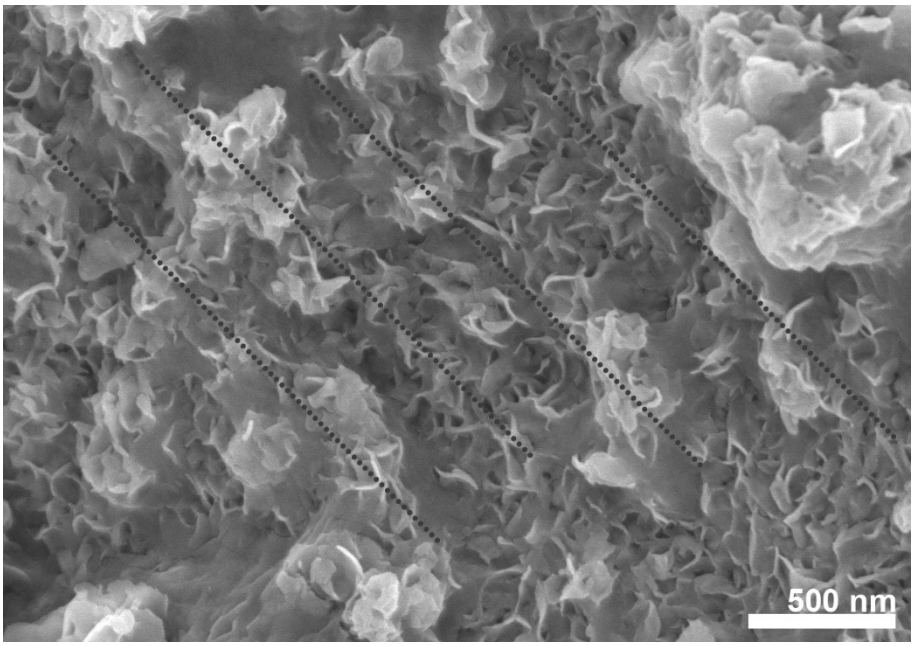

Figure S2. SEM images of MXene/$MoS_{2-x}P_x$ heterostructure.

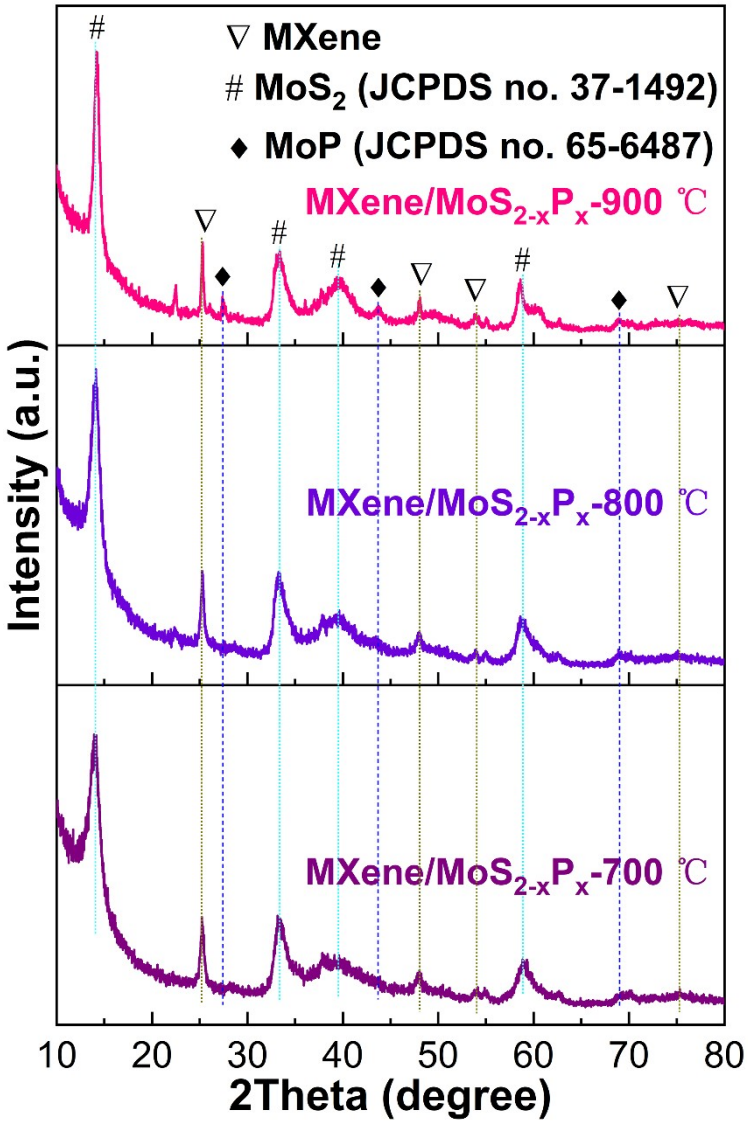

Figure S3. XRD patterns of MXene/$MoS_{2-x}P_x$ heterostructure phosphorized at 700, 800, and 900 Celsius.

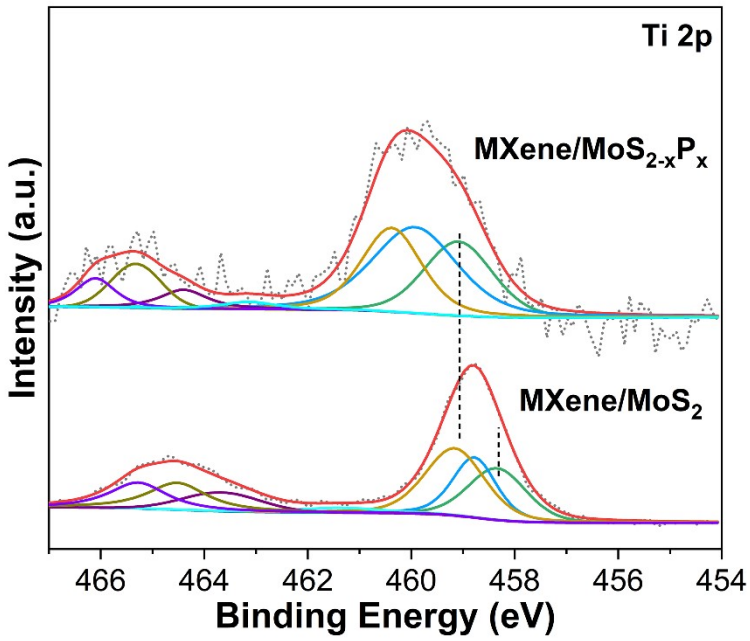

Figure S4. Ti 2p XPS spectra of MXene/MoS_2 and MXene/$MoS_{2-x}P_x$ heterostructures.

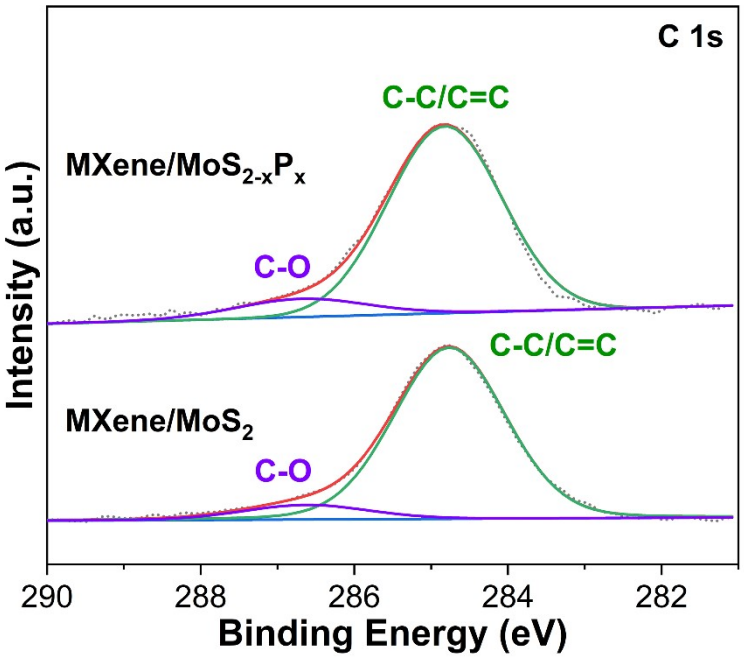

Figure S5. C 1s XPS spectra of MXene/MoS_2 and MXene/$MoS_{2-x}P_x$ heterostructures.

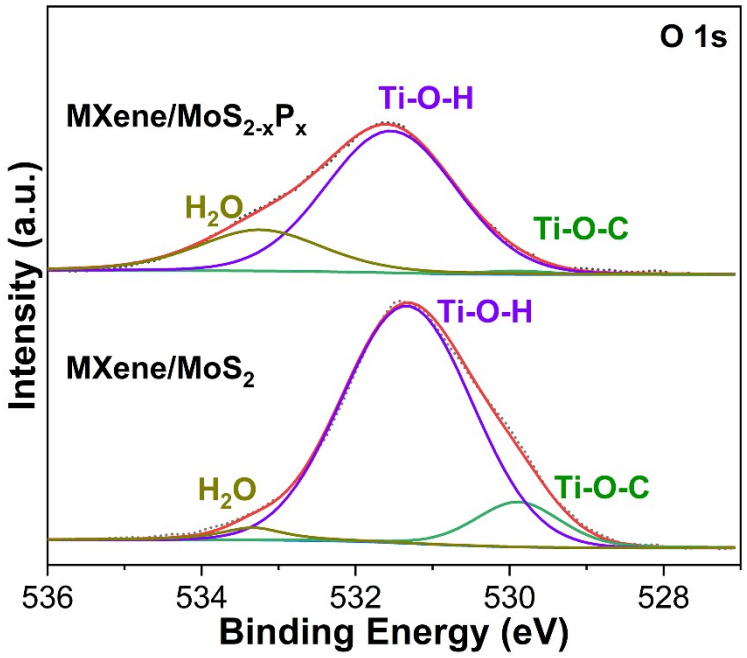

Figure S6. O 1s XPS spectra of MXene/MoS_2 and MXene/$MoS_{2-x}P_x$ heterostructures.

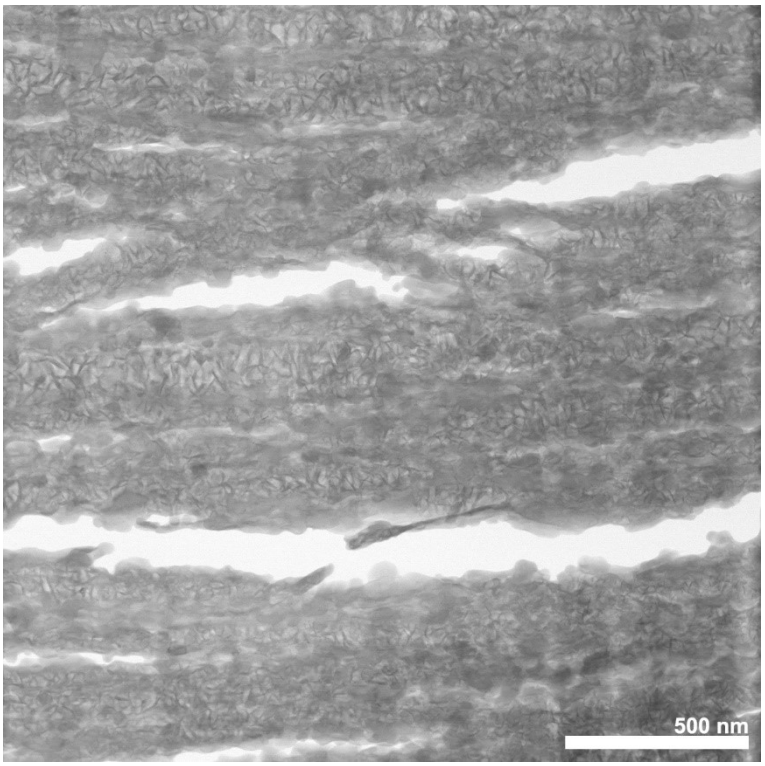

Figure S7. STEM image of MXene/MoS_2 heterostructure.

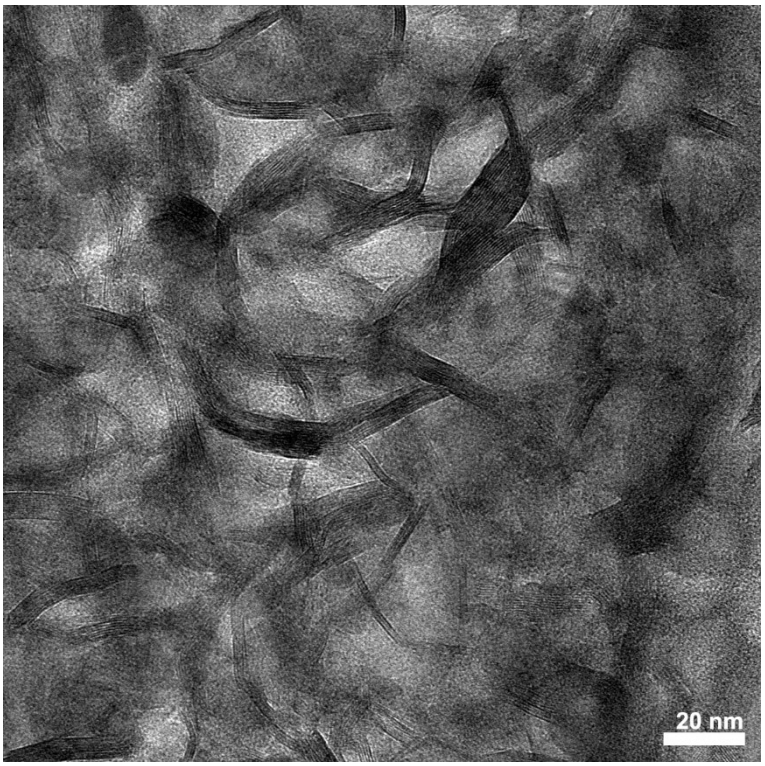

Figure S8. TEM image of MXene/MoS_2 heterostructure.

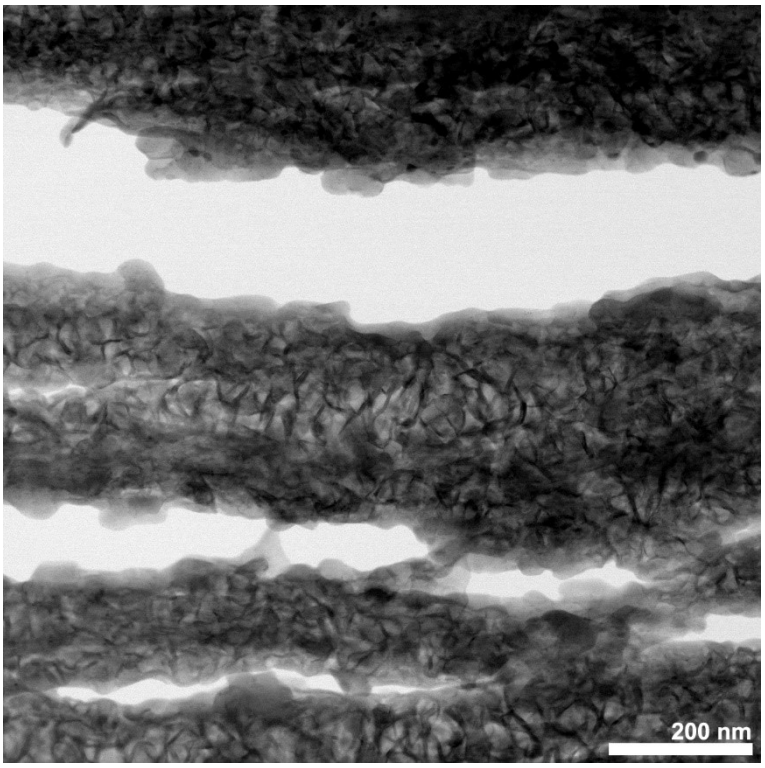

Figure S9. STEM image of MXene/MoS_2 heterostructure.

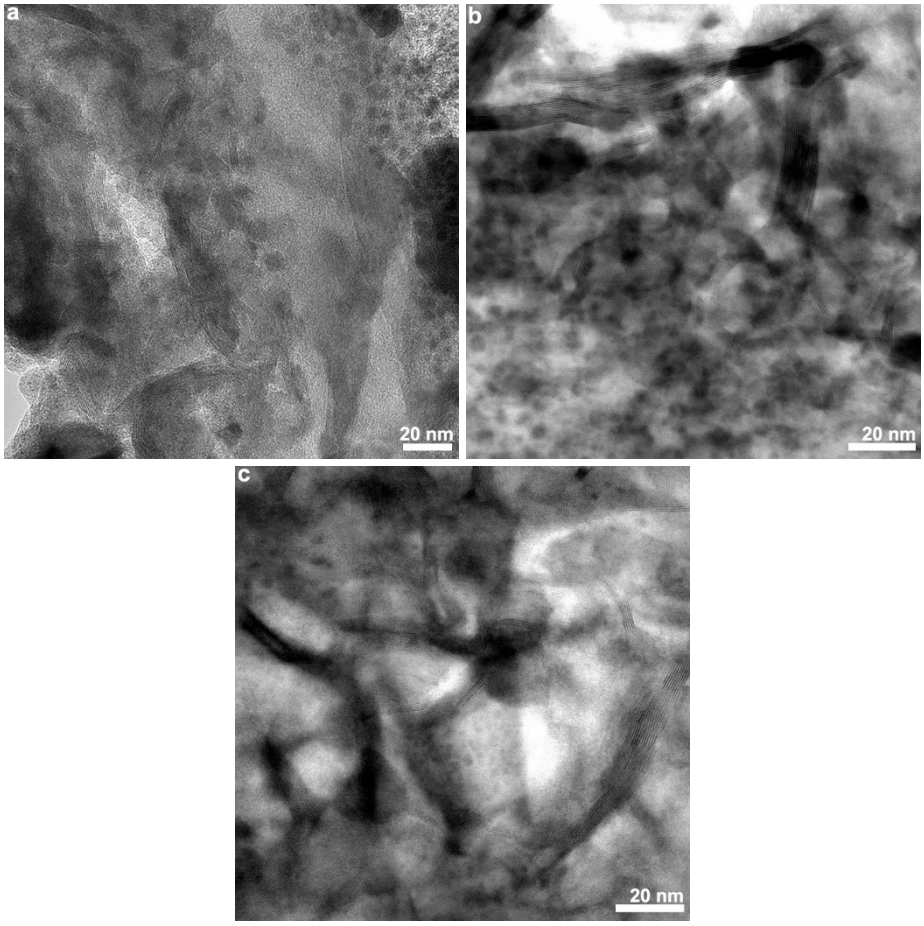

Figure S10. STEM image of MXene/MoS_2 heterostructure.

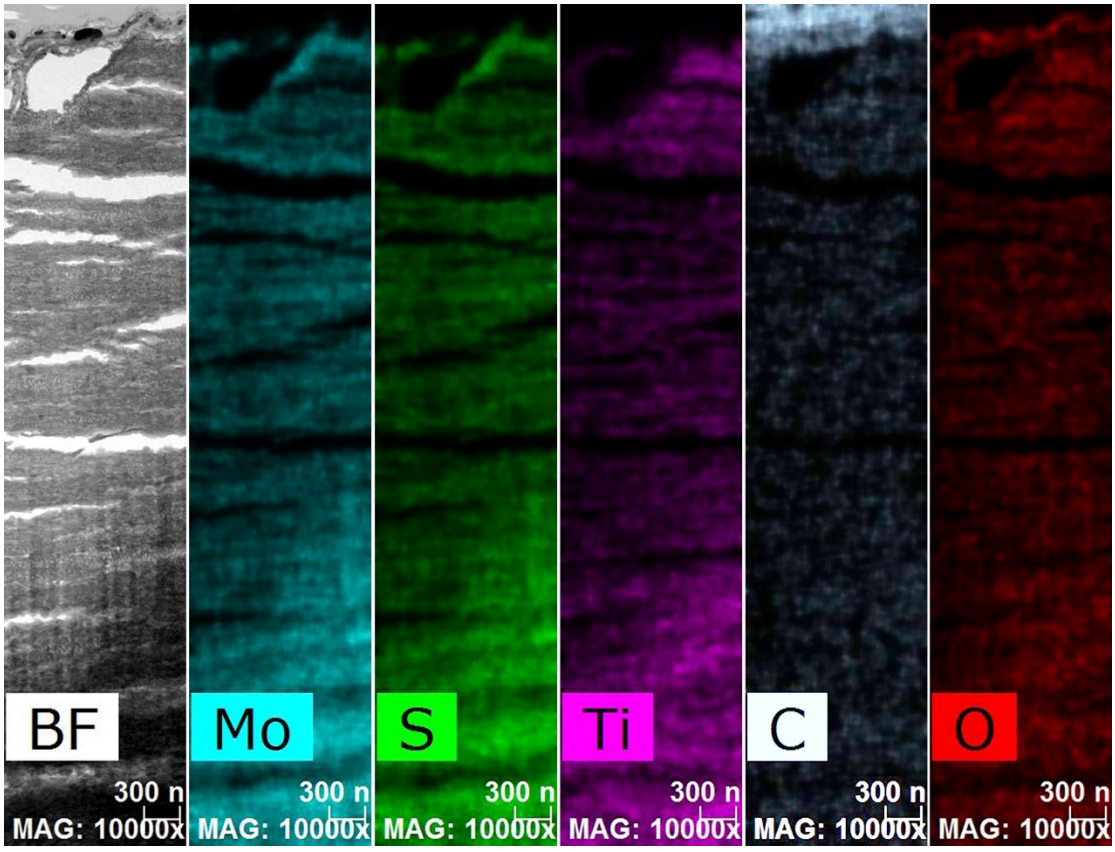

Figure S11. Elemental mapping images of MXene/MoS_2 heterostructure.

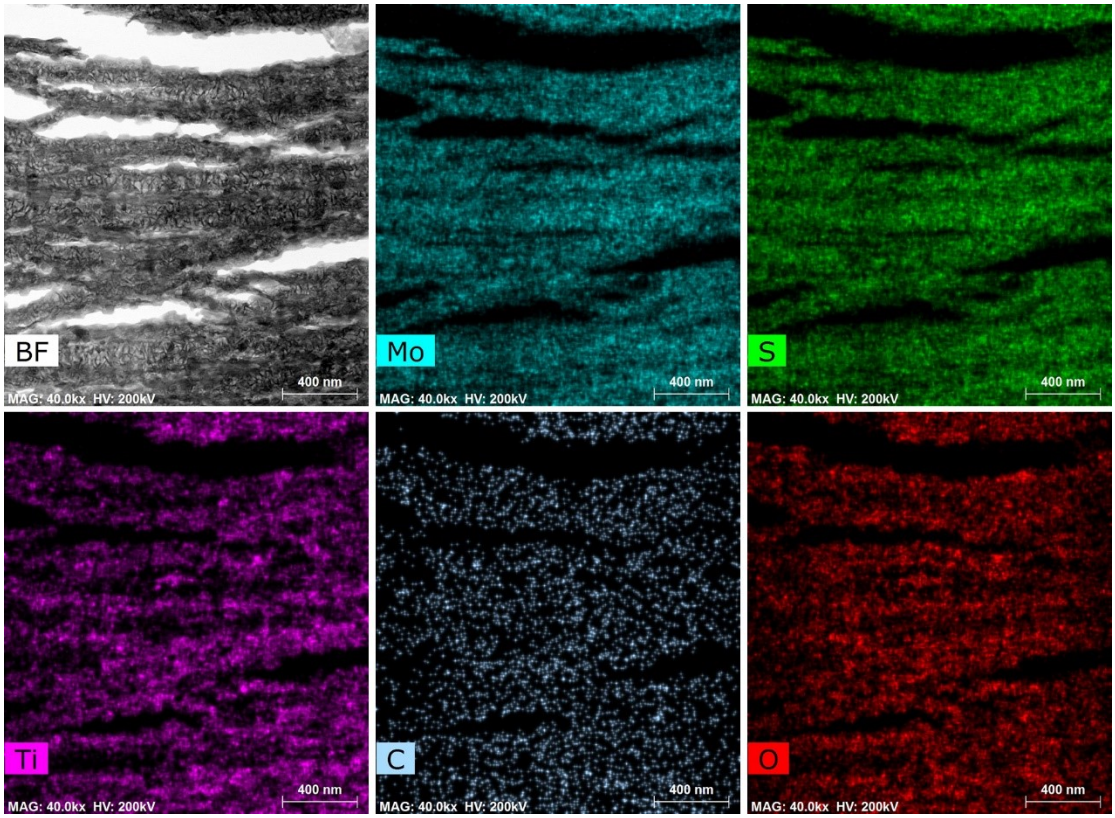

Figure S12. Elemental mapping images of MXene/MoS_2 heterostructure.

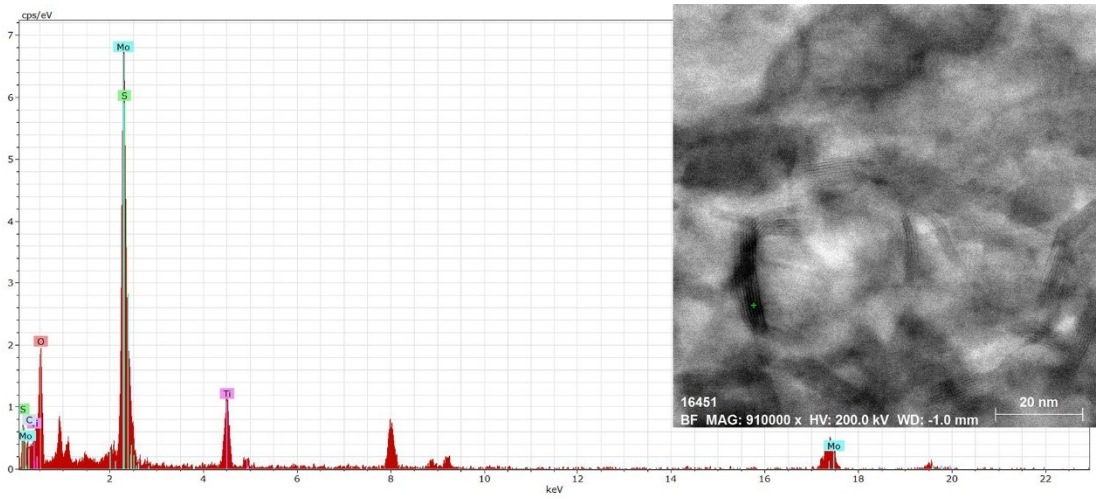

Figure S13. EDS spectroscopy of MXene/MoS_2 heterostructure.

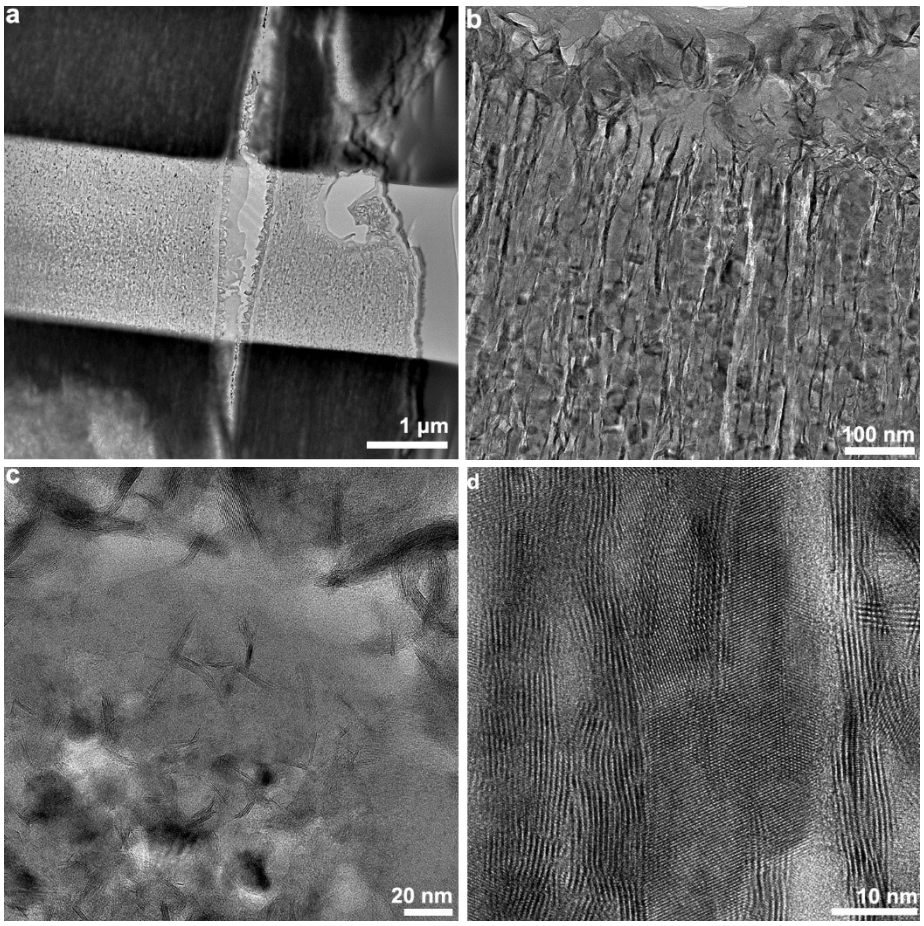

Figure S14. (a-c) STEM and (d) HRTEM imagse of MXene/$MoS_{2-x}P_x$ heterostructure.

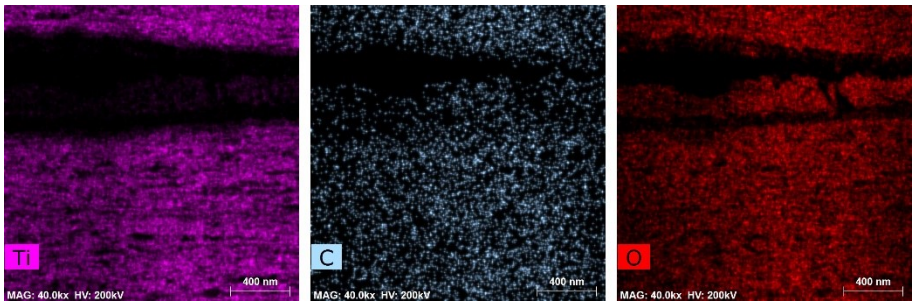

Figure S15. Elemental mapping images of Ti, C, and O for MXene/$MoS_{2-x}P_x$ heterostructure.

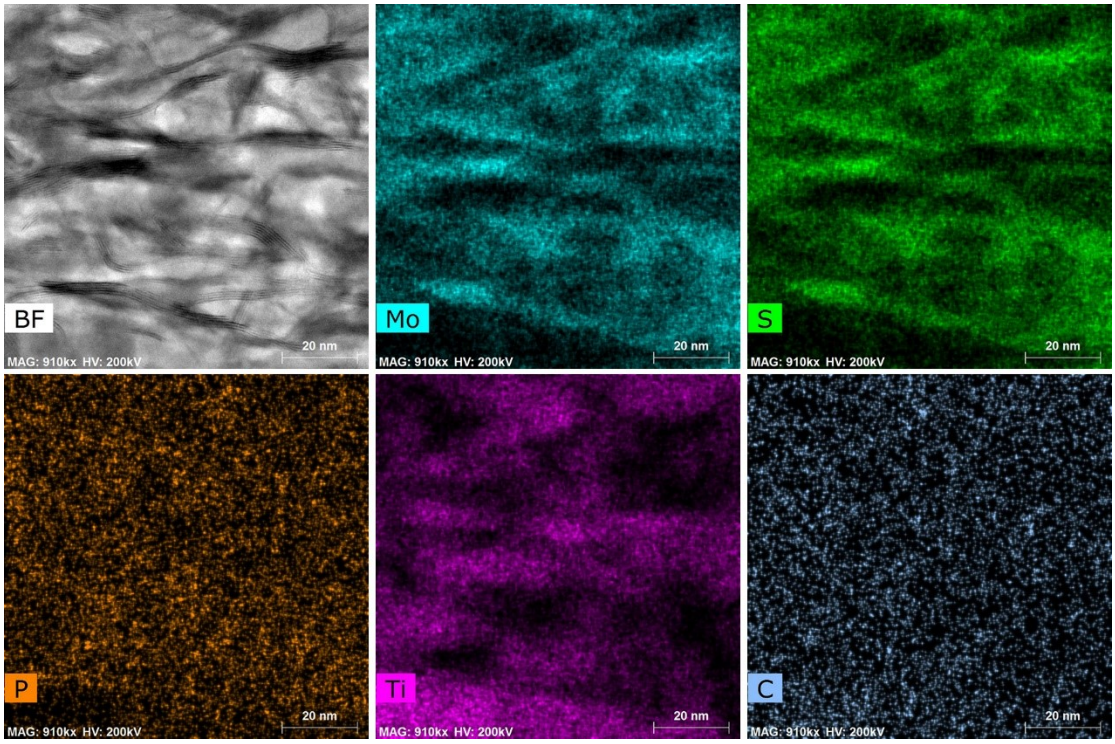

Figure S16. Elemental mapping images of MXene/$MoS_{2-x}P_x$ heterostructure.

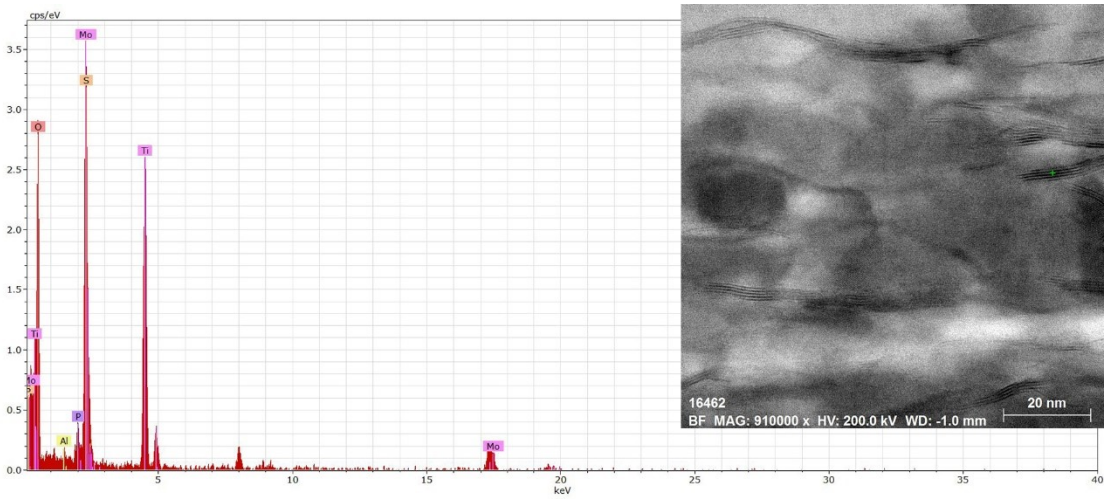

Figure S17. EDS spectrum of MXene/$MoS_{2-x}P_x$ heterostructure.

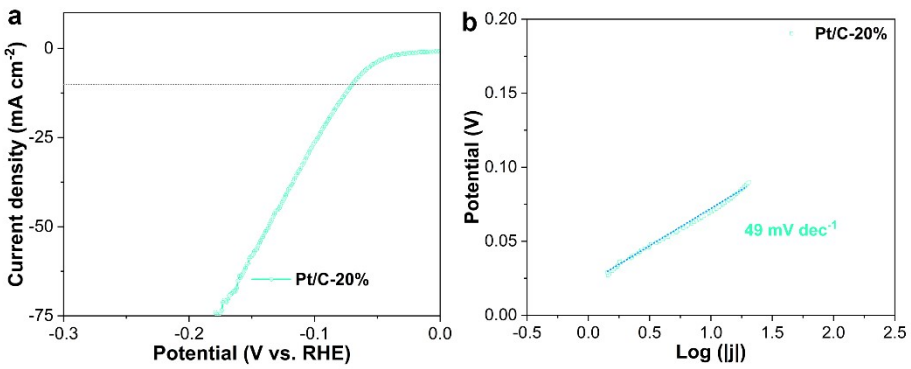

Figure S18. (a) HER polarization curves and (b) corresponding Tafel slope of Pt/C-20%.

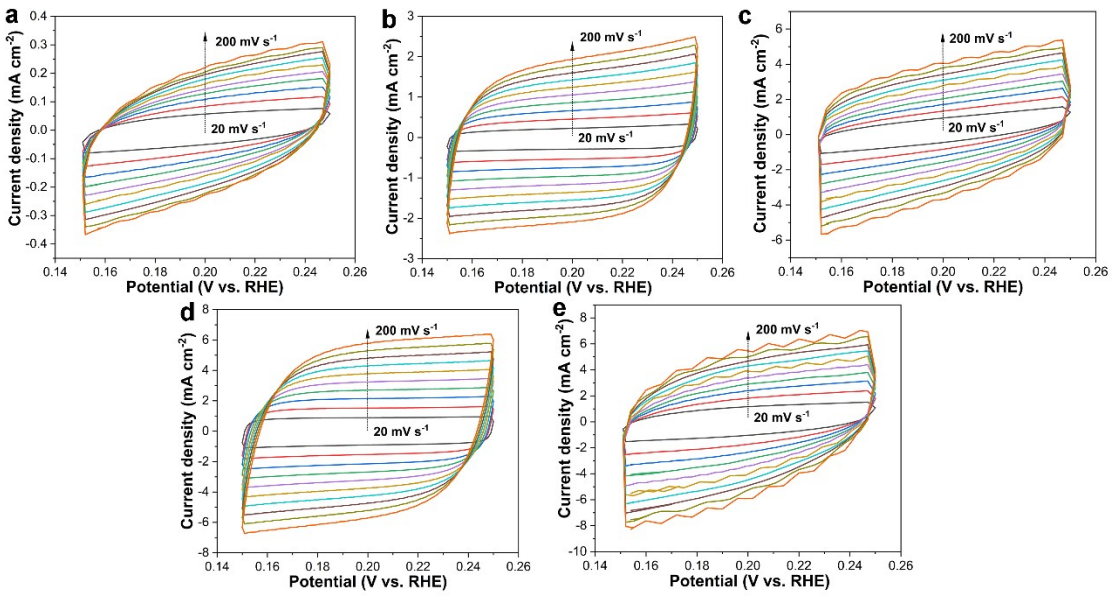

Figure S19. CV curve in a non-Faradaic potential region (0.15~0.25 V vs RHE) under different scan rates of (a) MXene, (b) MXene/MoS_2, and MXene/$MoS_{2-x}P_x$ heterostructure phosphated at (c) 700 ℃, (d) 800 ℃, and (f) 900 ℃.

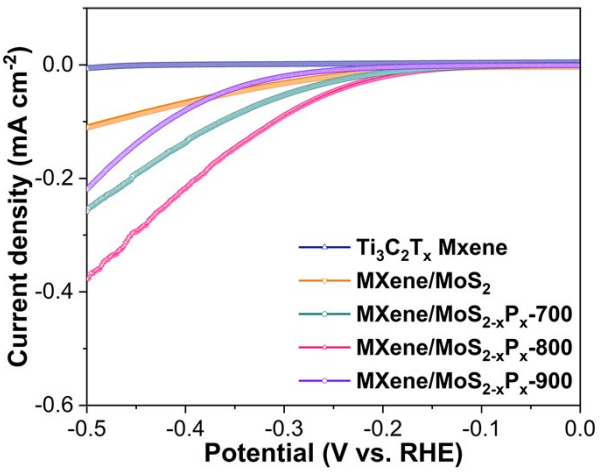

Figure S20. ECSA-normalized LSV curves of MXene, MXene/MoS_2, and MXene/$MoS_{2-x}P_x$ heterostructure phosphated at 700 ℃, 800 ℃, and 900 ℃. The C_{dl} can be converted into ECSA using the specific capacitance value for a flat surface of 0.035 mF cm^{-2} according to ECSA = C_{dl} / 0.035 mF cm^{-2}.

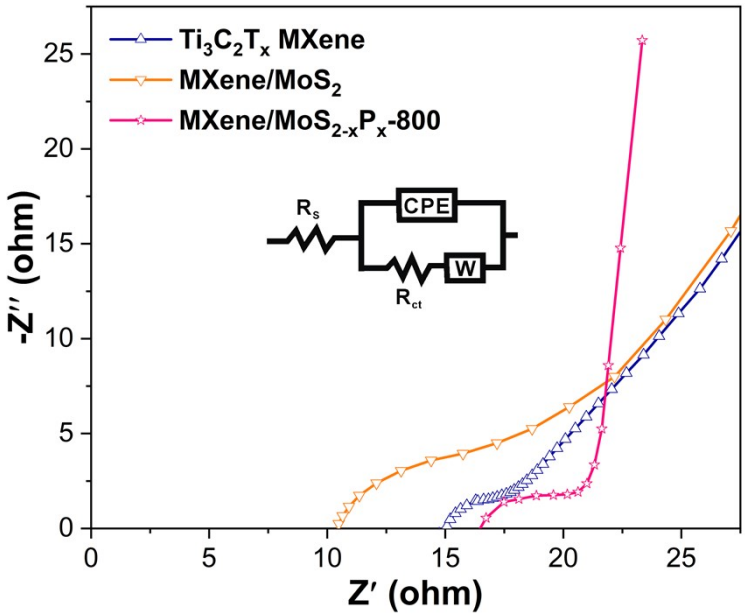

Figure S21. Nyquist EIS spectra of MXene, MXene/MoS_2, and MXene/$MoS_{2-x}P_x$ heterostructure.

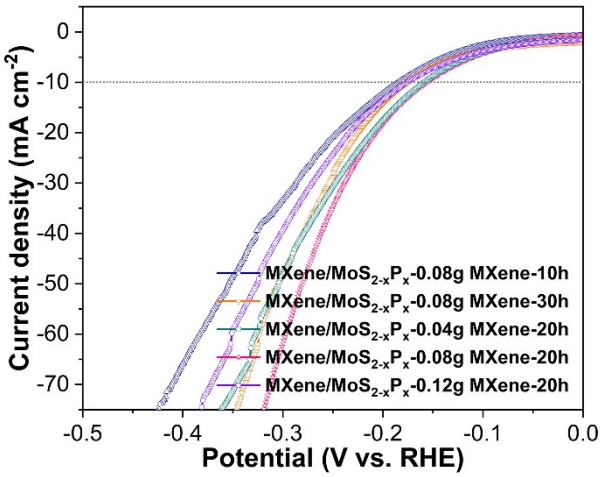

Figure S22. HER polarization curve of as-synthesized MXene/$MoS_{2-x}P_x$ heterostructure with different hydrothermal reaction time (10 h, 20 h, and 30 h) and MXene mass (0.04 g, 0.08 g, and 0.12 g).

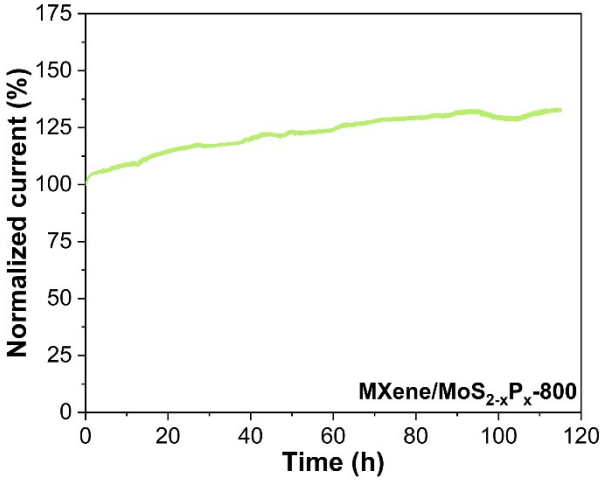

Figure S23. Long-term stability of MXene/$MoS_{2-x}P_x$ at -0.281 V (vs. RHE, applied potential at 50 mA cm^{-2}) for 115 h.

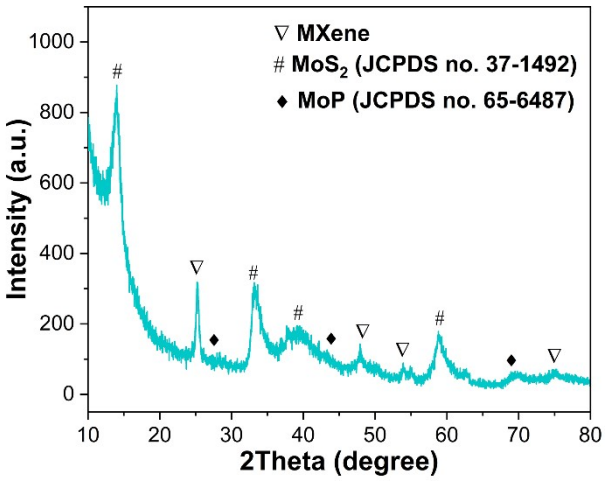

Figure S24. XRD pattern of MXene/$MoS_{2-x}P_x$ heterostructure after the long-term stability test (12 h).

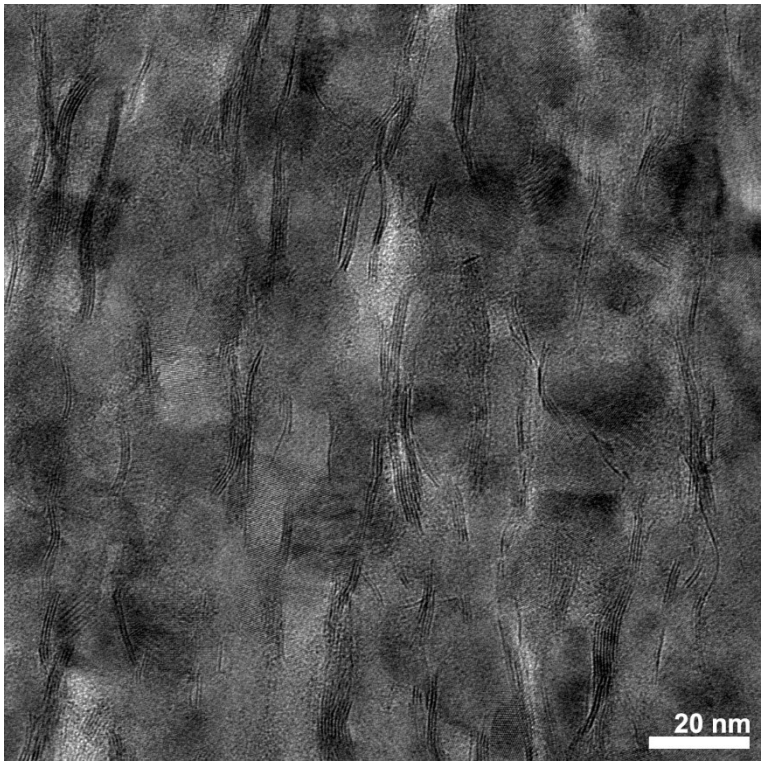

Figure S25. HRTEM images of MXene/$MoS_{2-x}P_x$ heterostructure after the long-term stability test (12 h).

Table S1. Element contents in the MXene/MoS_2 and MXene/$MoS_{2-x}P_x$ heterostructures detected by XPS technique.

Elements	Atomic %	
	MXene/MoS_2	MXene/$MoS_{2-x}P_x$
C	31.85	25.12
S	16.46	31.14
Mo	13.03	18.88
Ti	2.79	1.26
O	35.87	19.24
P	-	4.37

Table S2. Electrocatalytic performances toward HER of MXene/$MoS_{2-x}P_x$ and recently advanced non-noble-based catalysts.

Electrocatalysts	Loading (mg cm^{-2})	HER η (mV) @10 mA cm^{-2}	Electrolyte	Ref.
WS_2	0.283	337.0	0.5 M H_2SO_4	1
$RuTe_2$ alloy	0.203	245.0	0.5 M H_2SO_4	2
C_3N_4@NG	-	240.0	0.5 M H_2SO_4	3
MoS_2	-	240.0	0.5 M H_2SO_4	4
$CoS_{1.097}/MoS_2$	0.170	228.0	0.5 M H_2SO_4	5
Ni-P	-	222.0	0.5 M H_2SO_4	6
MoS_2-2C	0.500	217.0	0.5 M H_2SO_4	7
Co/MoS_{2-x}	-	210.0	0.5 M H_2SO_4	8
Fe,Al-$NiSe_2$/rGO	-	197.0	0.5 M H_2SO_4	9
Ag@MoS_2	0.010	195.7	0.5 M H_2SO_4	10
P-MoS_2	0.200	194.0	0.5 M H_2SO_4	11
Co_9S_8	-	193.0	0.5 M H_2SO_4	12

$Cr_{0.4}Mo_{0.6}B_2$	-	192.0	0.5 M H_2SO_4	13
CoSAs-MoS_2/TiN	-	187.5	0.5 M H_2SO_4	14
Ni_2P@C	0.540	186.0	0.5 M H_2SO_4	15
$MoSe_2$-ts@MoS_2-ts-c		186.0	0.5 M H_2SO_4	16
Co@NG	-	182.0	0.5 M H_2SO_4	17
Mo_2C@PC	0.410	177.0	0.5 M H_2SO_4	18
SV-MoS_2	-	170.0	0.5 M H_2SO_4	19
2H-$MoSe_2$	-	170.0	0.5 M H_2SO_4	20
P-MoO_{3-x}	0.285	166.0	0.5 M H_2SO_4	21
NC@$MoSe_2$	-	164.0	0.5 M H_2SO_4	22
WS_2	0.390	162.0	0.5 M H_2SO_4	23
Mo_2C@ng/CNT	-	160.0	0.5 M H_2SO_4	24
MoP	0.860	158.0	0.5 M H_2SO_4	25
MXene/$MoS_{2-x}P_x$	0.200	157.0	0.5 M H_2SO_4	This work
rGO/SiO_2	-	134.0	0.5 M H_2SO_4	26
PSS-MoS_2/CNT	-	114.0	0.5 M H_2SO_4	27
Pd-TiO_2	0.500	108.0	0.5 M H_2SO_4	28
Pt_1@Fe-N-C	0.400	60.0	0.5 M H_2SO_4	2 9
RhP_x@NPC	0.125	22.0	0.5 M H_2SO_4	30

References

1 W. L. Liu, J. Benson, C. Dawson, A. Strudwick, A. P. A. Raju, Y. S. Han, M. X. Li and P. Papakonstantinou, *Nanoscale*, 2017, **9**, 13515-13526.

2 J. Wang, L. L. Han, B. L. Huang, Q. Shao, H. L. Xin and X. Q. Huang, *Nat. Commun.*, 2019, **10**, 5692.

3 Y. Zheng, Y. Jiao, Y. Zhu, L. H. Li, Y. Han, Y. Chen, A. Du, M. Jaroniec and S. Z.

Qiao, *Nat. Commun.*, 2014, **5**, 3783.

4 X. Y. Qian, K. Xie, S. Y. Guo, Q. H. Liang, S. L. Zhang, Z. Y. Xiong, H. L. Zhan, C. C. Liu, X. W. Yang, J. W. Zhu and D. Li, *Chem. Commun.*, 2020, **56**, 7005-7008.

5 J. P. Sun, Z. D. Huang, T. X. Huang, X. K. Wang, X. Wang, P. Y. Yu, C. Zong, F. N. Dai and D. F. Sun, *ACS Appl. Energy Mater.*, 2019, **2**, 7504-7511.

6 R. N. Wasalathanthri, S. Jeffrey, N. Su, K. Sun and D. M. Giolando, *ChemistrySelect*, 2017, **2**, 8020-8027.

7 J. Xu, X. J. Cui, Z. W. Fan, X. X. Zhu, W. Guo, Z. Z. Xie, D. Liu, D. Y. Qu, H. L. Tang and J. S. Li, *Mater. Adv.*, 2021, DOI: 10.1039/D1MA00681A.

8 S. Park, J. Park, H. Abroshan, J. M. Zhang, J. H. Guo, S. Siahrostami and X. L. Zheng, *ACS Energy Lett.*, 2018, **3**, 2685-2693.

9 L. L. Chen, H. Jang, M. G. Kim, Q. Qin, X. E. Liu and J. Cho, *Nanoscale*, 2020, **12**, 13680-13687.

10 J. Z. Chen, G. G. Liu, Y.-Z. Zhu, M. Su, P. F. Yin, X.-J. Wu, Q. P. Lu, C. L. Tan, M. T. Zhao, Z. Q. Liu, W. M. Yang, H. Li, G.-H. Nam, L. P. Zhang, Z. H. Chen, X. Huang, P. M. Radjenovic, W. Huang, Z.-Q. Tian, J.-F. Li and H. Zhang, *J. Am. Chem. Soc.*, 2020, **142**, 7161-7167.

11 W. Z. Wu, C. Y. Niu, C. Wei, Y. Jia, C. Li and Q. Xu, *Angew. Chem. Int. Ed*., 2019, **58**, 2029-2033.

12 H. Y. Mou, Z. M. Xue, B. L. Zhang, X. Lan and T. C. Mu, *J. Mater. Chem. A*, 2021, **9**, 2099-2103.

13 H. Park, E. Lee, M. Lei, H. Joo, S. Coh and B. P. T. Fokwa, *Adv. Mater.*, 2020, **32**,

202000855.

14 T. L. L. Doan, D. C. Nguyen, S. Prabhakaran, D. H. Kim, D. T. Tran, N. H. Kim and J. H. Lee, *Adv. Funct. Mater.*, 2021, **31**, 2100233.

15 S. Q. He, S. Y. He, F. Gao, X. Bo, Q. X. Wang, X. J. Chen, J. J. Duan and C. Zhao, *Appl. Surf. Sci.*, 2018, **457**, 933-941.

16 M. D. Sharma, C. Mahala and M. Basu, *Inorg. Chem.*, 2020, **59**, 4377-4388.

17 X. D. Wen, L. Bai, M. Li and J. Q. Guan, *ACS Sustainable Chem. Eng.*, 2019, **7**, 9249-9256.

18 J. Yang, F. J. Zhang, X. Wang, D. S. He, G. Wu, Q. H. Yang, X. Hong, Y. E. Wu and Y. D. Li, *Angew. Chem.*, 2016, **128**, 13046-13050.

19 H. Li, C. Tsai, A. L. Koh, L. L. Cai, A. W. Contryman, A. H. Fragapane, J. H. Zhao, H. S. Han, H. C. Manoharan, F. Abild-Pedersen, J. K. Nørskov and X. L. Zheng, *Nat. Mater.*, 2016, **15**, 48-53.

20 Y. S. Chang, C. Y. Chen, C. J. Ho, C. M. Cheng, H. R. Chen, T. Y. Fu, Y. T. Huang, S. W. Ke, H. Y. Du, K. Y. Lee, L. C. Chao, L. C. Chen, K. H. Chen, Y. W. Chu and R. S. Chen, *Nano Energy*, 2021, **84**, 105922.

21 L. Li, T. Zhang, J. Q. Yan, X. D. Cai and S. Z. (Frank) Liu, *Small*, 2017, **13**, 1700441.

22 W. H. Chen, R. Qiao, C. S. Song, L. H. Zhao, Z.-J. Jiang, T. Maiyalagan and Z. Q. Jiang, *J. Catal.*, 2020, **381**, 363-373.

23 I. H. Kwak, I. S. Kwon, J. H. Lee, Y. R. Lim and J. Park, *J. Mater. Chem. C*, 2021, **9**, 101-109.

24 C. F. Yang, K. Shen, R. Zhao, H. Xiang, J. Wu, W. D. Zhong, Q. Zhang, X. K. Li and N. J. Yang, *Adv. Funct. Mater.*, 2021, 2108167.

25 P. Xiao, M. A. Sk, L. Thia, X. M. Ge, R. J. Lim, J.-Y. Wang, K. H. Lim and X. Wang, *Energy Environ. Sci.*, 2014, **7**, 2624-2629.

26 Y. J. Huang, M. Wang, Y. Li, S. J. Yin, H. W. Zhu and C. L. Wan, *Small Methods*, 2021, **5**, 2100621.

27 P. F. Wang, Y. X. Dai, X. Y. Wang, X. Ren and C. N. Luo, *ChemElectroChem*, 2021, **8**, 2259-2265.

28 X. J. Zeng, Y. C. Bai, S. M. Choi, L. J. Tong, R. M. Aleisa, Z. W. Li, X. F. Liu, R. H. Yu, N. V. Myung and Y. D. Yin, *Mater. Today Nano*, 2019, **6**, 100038.

29 X. J. Zeng, J. L. Shui, X. F. Liu, Q. T. Liu, Y. C. Li, J. X. Shang, L. R. Zheng and R. H. Yu, *Adv. Energy Mater.*, 2018, **8**, 1701345.

30 J. Q. Chi, X. J. Zeng, X. Shang, B. Dong, Y. M. Chai, C. G. Liu, M. Marin and Y. D. Yin, *Adv. Funct. Mater.*, 2019, **29**, 1901790.